



Catalysis  
Science &  
Technology

**Comparison of SiO<sub>2</sub>-Supported Molybdena, Tungsta and Rhenia Catalysts for Olefin Metathesis**

Journal:	<i>Catalysis Science &amp; Technology</i>
Manuscript ID	CY-ART-06-2024-000730.R1
Article Type:	Paper
Date Submitted by the Author:	14-Jul-2024
Complete List of Authors:	Zhang, Bin; Lehigh University, Chemical & Biomolecular Engineering Wachs, Israel; Lehigh University, Chemical Engineering

SCHOLARONE™  
Manuscripts

## ARTICLE

# Comparison of SiO<sub>2</sub>-Supported Molybdena, Tungsta and Rhenia Catalysts for Olefin Metathesis

Received 00th January 20xx,  
Accepted 00th January 20xx

Bin Zhang, Israel E. Wachs

DOI: 10.1039/x0xx00000x

The characteristics of supported MO<sub>x</sub>/SiO<sub>2</sub> catalysts (M = Re, Mo, W) for olefin metathesis were compared side-by-side to understand the differences among these catalyst systems. The series of SiO<sub>2</sub>-supported metal oxide (ReO<sub>x</sub>, MoO<sub>x</sub>, WO<sub>x</sub>) catalysts, with maximum achievable dispersion of surface MO<sub>x</sub> sites, was synthesized by incipient-wetness impregnation of the corresponding aqueous precursors, molecularly characterized (*in situ* Raman and DRIFTS), chemically probed with transient studies (C<sub>3</sub>H<sub>6</sub>-TPSR-MS, C<sub>3</sub>H<sub>6</sub>-TPSR-IR, and C<sub>2</sub>H<sub>4</sub>/2-C<sub>4</sub>H<sub>8</sub> titration with C<sub>2</sub>H<sub>4</sub>-TPSR-MS) and steady state activity for C<sub>3</sub>H<sub>6</sub> metathesis. Under dehydrated conditions, the initial SiO<sub>2</sub>-supported surface metal oxide sites are fully dispersed as isolated sites on SiO<sub>2</sub> and present as isolated tri-oxo (O=)<sub>3</sub>ReO sites, isolated di-oxo (O=)<sub>2</sub>MoO<sub>2</sub> sites and a mixture of isolated di-oxo (O=)<sub>2</sub>WO<sub>2</sub> and mono-oxo (O=)WO<sub>4</sub> sites (dioxo >> mono-oxo) anchored at the isolated Si-OH surface hydroxyls of SiO<sub>2</sub> support. High temperature propylene pre-treatments were required to activate the SiO<sub>2</sub>-supported MO<sub>x</sub> catalysts, but also resulted in MO<sub>x</sub> volatilization (ReO<sub>x</sub> > MoO<sub>x</sub> >> WO<sub>x</sub>). The number of activated surface MO<sub>x</sub> sites and TOF values varied with the specific MO<sub>x</sub> site, activation temperatures and reaction temperatures, which are related to the stability of the surface M=O oxo and M=Carbene bonds. The higher thermal stability, activity and TOF of the surface WO<sub>x</sub> sites on SiO<sub>2</sub> at elevated temperatures relative to the supported ReO<sub>x</sub>/SiO<sub>2</sub> and MoO<sub>x</sub>/SiO<sub>2</sub> catalysts account for adoption of the supported WO<sub>x</sub>/SiO<sub>2</sub> catalyst as the industrial olefin metathesis catalyst among these supported MO<sub>x</sub>/SiO<sub>2</sub> catalysts.

Keywords: metathesis, propylene, silica, molybdena, rhenia, tungsta, Raman, DRIFTS, TPSR, activation

## 1. Introduction

There is a growing gap between the global supply and demand of propylene attributed to a feedstock shift from steam cracking of natural gas and oil refinery operation. The olefin metathesis reaction is considered a promising approach to address the global shortage of propylene by cleaving and rearranging the C=C bonds in ethylene and 2-butene. Among olefin metathesis catalysts employed in industry, high surface area oxide supported-MO<sub>x</sub> (M = Re, Mo, W) catalysts have attracted substantial research attention due to their high activity and selectivity.<sup>1</sup> Among these catalysts, only the SiO<sub>2</sub>-supported WO<sub>x</sub> catalyst is the preferred propylene metathesis catalysts of small olefins in industrial practice (Philips Triolefin Process and Lummus Olefin Conversion Technology)<sup>2-3</sup>, while SiO<sub>2</sub>-supported ReO<sub>x</sub> and MoO<sub>x</sub> catalysts are essentially not industrially employed.<sup>4-5</sup> Previous studies found that the supported ReO<sub>x</sub>/Al<sub>2</sub>O<sub>3</sub> catalyst is highly active for propylene metathesis at ambient temperature, while the supported ReO<sub>x</sub>/SiO<sub>2</sub> catalyst is difficult to activate.<sup>6-7</sup> The supported MoO<sub>x</sub>/SiO<sub>2</sub> catalyst is also reported to require high

temperatures (>400 °C) for activation with propylene<sup>8-9</sup> and is about an order of magnitude less active than the supported MoO<sub>x</sub>/Al<sub>2</sub>O<sub>3</sub> catalyst used for Shell Higher Olefin Process.<sup>1,10</sup> The supported WO<sub>x</sub>/SiO<sub>2</sub> catalyst is a major industrial propylene metathesis catalyst that operates at 400-600°C and also requires high temperature pre-activation with propylene.<sup>11</sup> Although the supported WO<sub>x</sub>/SiO<sub>2</sub> catalyst exhibits a longer lifetime than the corresponding supported ReO<sub>x</sub> and MoO<sub>x</sub> catalysts,<sup>11</sup> a direct comparison of the catalytic surface active sites (molecular structure, anchoring sites, activation, number of activated sites, thermal stability, activity and TOF values for propylene self-metathesis) of SiO<sub>2</sub> supported transition metal oxide catalysts is still lacking and needed to better understand the superior properties of the supported WO<sub>x</sub>/SiO<sub>2</sub> catalyst system.

The objective of this study is to investigate the behavior of the surface ReO<sub>x</sub>, MoO<sub>x</sub> and WO<sub>x</sub> sites on SiO<sub>2</sub> during activation with propylene and during propylene metathesis. Although the oxide support was found to have a pronounced effect on the activation and catalytic activities of supported MO<sub>x</sub> catalysts,<sup>6,13</sup> the present study only focuses on supported MO<sub>x</sub>/SiO<sub>2</sub> catalysts in order to obtain fundamental insights into the behavior of the commercial-type supported WO<sub>x</sub>/SiO<sub>2</sub> catalyst compared to the corresponding supported ReO<sub>x</sub>/SiO<sub>2</sub> and MoO<sub>x</sub>/SiO<sub>2</sub> catalysts by their side-by-side comparison. The SiO<sub>2</sub>-supported catalysts were characterized with *in situ*

*Operando Molecular Spectroscopy and Catalysis Laboratory, Department of Chemical & Biomolecular Engineering, Lehigh University, Bethlehem, PA, 18015, United States*

† Electronic Supplementary Information (ESI) available: [details of any supplementary information available should be included here]. See DOI: 10.1039/x0xx00000x

Raman and DRIFTS and chemically probed with transient (double  $\text{C}_3\text{H}_6$ -TPSR-MS, double *in situ*  $\text{C}_3\text{H}_6$ -TPSR-IR,  $\text{C}_2\text{H}_4/2\text{-C}_4\text{H}_8$  titration followed with  $\text{C}_2\text{H}_4$ -TPSR-MS) and steady state self-metathesis of propylene. This is the first time the similarities and differences of the supported  $\text{ReO}_x$ ,  $\text{MoO}_x$  and  $\text{WO}_x$  sites on the same metal oxide support ( $\text{SiO}_2$ ) have been compared for propylene metathesis. The side-by-side comparison of these  $\text{SiO}_2$ -supported transition metal oxide catalysts will examine the molecular structure, anchoring sites, activation, number of activated sites, thermal stability, activity and TOF values for propylene self-metathesis. The present investigation will provide insights about the reasons for the relative behavior of the  $\text{SiO}_2$ -supported  $\text{ReO}_x$ ,  $\text{MoO}_x$  and  $\text{WO}_x$  catalysts during propylene activation and self-metathesis of propylene. The reversibility of the propylene metathesis reaction ( $2 \text{C}_3\text{H}_6 \rightleftharpoons \text{C}_2\text{H}_4 + 2\text{-C}_4\text{H}_8$ ) assures that the reaction pathway proceeds similarly in the forward and reverse directions (microscopic reversibility), with also the same number of sites titratable in both directions.<sup>32-33</sup>

## II. Experimental Details

### Catalyst Synthesis.

The supported  $\text{ReO}_x$ ,  $\text{MoO}_x$  and  $\text{WO}_x$  catalysts were prepared by incipient-wetness impregnation (IWI) of aqueous perrenic acid ( $\text{HReO}_4$ , Alfa Aesar, 75-80%), aqueous ammonium heptamolybdate ( $(\text{NH}_4)_6\text{Mo}_7\text{O}_{24} \cdot 4\text{H}_2\text{O}$ , Alfa Aesar, 99%) and aqueous ammonium metatungstate hydrate ( $(\text{NH}_4)_6\text{H}_2\text{W}_{12}\text{O}_{40} \cdot x\text{H}_2\text{O}$ , Pfaltz and Bauer, 99.5%) into the  $\text{SiO}_2$  (Cabot, Cab-O-Sil, EH-5, 350  $\text{m}^2/\text{g}$ ) support. Prior to IWI, the  $\text{SiO}_2$  support was treated with  $\text{H}_2\text{O}$  to increase the number of surface hydroxyls and calcined in air at 500°C for 4h. After impregnation of the aqueous precursors, the supported catalysts were dried at room temperature overnight, then at 120°C for 2h in air before finally being calcined by ramping the temperature at 1°C/min in flowing air (100 mL/min) to 500°C and held at this temperature for 4h. Due to the poor reactivity of the  $\text{SiO}_2$  surface silanols, the maximum achieved loading (surface coverage) of  $\text{ReO}_x$ ,  $\text{MoO}_x$  and  $\text{WO}_x$  on the  $\text{SiO}_2$  support was 5.5%  $\text{ReO}_x$  ( $2.3 \times 10^{-4}$  mol Re atoms/g; 0.4 Re/ $\text{nm}^2$ ), 7.5%  $\text{MoO}_x$  ( $3.1 \times 10^{-4}$  mol Mo atoms/g; 0.9 Mo/ $\text{nm}^2$ ), and 6.0%  $\text{WO}_x$  ( $2.5 \times 10^{-4}$  mol W atoms/g; 0.5 W/ $\text{nm}^2$ ).

### *In situ* Diffuse Reflectance Infrared Fourier Transform Spectroscopy (DRIFTS).

The *in situ* DRIFTS spectra of  $\text{SiO}_2$ -supported metal oxide catalysts were collected with a Thermo Scientific Nicolet 8700 FT-IR spectrometer equipped with a Harrick Praying Mantis attachment (DRA-2 with  $\text{CaF}_2$  window). The collected spectra employed a Mercury-Cadmium-Telluride (MCT) detector having a resolution of 4  $\text{cm}^{-1}$  with an accumulation of 96 scans/min. About 20mg of catalyst powder was loaded into the *in situ* reaction cell (Harrick, HVC-DR2 with a  $\text{CaF}_2$  window) for DRIFTS spectral collection. A Brooks 5850E mass flow controller controlled the gas flow rate through the *in situ* cell. The procedure for collecting *in situ* DRIFTS spectra of dehydrated catalysts was as follows: the catalyst was heated at

10°C/min from room temperature to 500°C under flowing 10%  $\text{O}_2/\text{Ar}$  (Praxair, UHP, 30 mL/min) and held for 1 h, the temperature was subsequently cooled at 10°C/min to 120°C under flowing 10%  $\text{O}_2/\text{Ar}$ . The procedure for collecting *in situ*  $\text{C}_3\text{H}_6$ -TPSR-DRIFTS spectra is the same as described below for the  $\text{C}_3\text{H}_6$ -TPSR-MS studies.

### *In situ* Raman Spectroscopy.

The *in situ* Raman spectra of  $\text{SiO}_2$ -supported metal oxide catalysts were collected by a Horiba Labram HR Evolution spectrometer (442nm). The laser was focused on the catalysts with a confocal microscope equipped with an Olympus BX-30 X50 objective lens. A 900 grooves/nm grating was selected to optimize the spectral resolution to approximately 1  $\text{cm}^{-1}$ . Daily calibration of the Raman spectrometer employed a silicon standard having a reference peak of 520.7  $\text{cm}^{-1}$ . The same mass flow controllers as indicated above were used to monitor the gas flow rates. Approximately 20mg of catalysts powders were loaded into an *in situ* reaction cell (Harrick Scientific HVC-MRA-5) that was controlled by a pre-calibrated temperature controller (ATK-024-4). The thermocouple of the controller is in direct contact with the catalyst bed to obtain accurate temperature reading. The Raman spectra were collected with an accumulation of 3 scans (20s/scan) with a Horiba-Jobin Yvon CCD-3000 V CCD camera detector. The following procedure was employed for collecting the *in situ* Raman spectra: (1) the reaction cell was heated at 10°C/min in flowing 10%  $\text{O}_2/\text{Ar}$  (Praxair, UHP, 30 mL/min) to the dehydration/reaction temperatures (450°C ( $\text{ReO}_x/\text{SiO}_2$ ), 550°C ( $\text{MoO}_x/\text{SiO}_2$ ), 650°C ( $\text{WO}_x/\text{SiO}_2$ )) and held for 60min at the final indicated temperatures, (2) the flowing gas was switched to 5%  $\text{C}_3\text{H}_6/\text{Ar}$  (Praxair, Purity 99%, 30 mL/min) for 90min at the reaction temperature, and (3) the catalysts were re-oxidized with 10%  $\text{O}_2/\text{Ar}$  (Praxair, UHP, 30 mL/min) at the dehydration temperature for 60 min. The internal standard for normalization of the Raman spectra was the Raman band of the  $\text{SiO}_2$  support at  $\sim 607 \text{ cm}^{-1}$ . The dehydration, activation and re-oxidation temperatures were determined from the 1<sup>st</sup>  $\text{C}_3\text{H}_6$ -TPSR-MS findings given below.

### $\text{C}_3\text{H}_6$ -Temperature Programmed Surface Reaction (TPSR)-MS.

The  $\text{C}_3\text{H}_6$ -TPSR-MS measurements were performed on the Altamira Instruments system (AMI-200). Approximately 0.1g of catalyst powder was loaded into a U-tube quartz reactor and placed in the AMI-200 system. The dehydration procedure was the same as indicated above for the Raman experiments. Following catalyst dehydration, Ar (Air Gas, UHP, 30 mL/min) was first flown through the reactor at 30°C for 30 minutes and followed by two  $\text{C}_3\text{H}_6$ -TPSR cycles: (1) in the 1<sup>st</sup> cycle, 5%  $\text{C}_3\text{H}_6/\text{Ar}$  (Praxair, Purity 99%, 30 mL/min) was initially flown and held at 30°C for several minutes to stabilize the MS signal and the reactor was subsequently heated at 10°C/min to 600°C ( $\text{ReO}_x/\text{SiO}_2$ ,  $\text{MoO}_x/\text{SiO}_2$ ) and 800°C ( $\text{WO}_x/\text{SiO}_2$ ); and (2) in the 2<sup>nd</sup> cycle, the reactor was cooled to room temperature with flowing Ar (Air Gas, UHP, 30 mL/min), switched to 5%  $\text{C}_3\text{H}_6/\text{Ar}$  (Praxair, Purity 99%, 30 mL/min) and heated again at 10°C/min to 600°C ( $\text{ReO}_x/\text{SiO}_2$ ,  $\text{MoO}_x/\text{SiO}_2$ ) and 800°C ( $\text{WO}_x/\text{SiO}_2$ ). The

higher reaction temperature for  $\text{WO}_x/\text{SiO}_2$  was employed because olefin metathesis with this catalyst required higher activation and reaction temperatures. The outlet of the reactor was connected to an online quadrupole mass spectrometer (MS, Dycor ProLine Process) to measure the exiting gases. The following mass/charge ratio channels were used for analysis of propylene and the reaction products:  $m/z=18$  ( $\text{H}_2\text{O}$ ),  $m/z=28$  ( $\text{CO}$ ),  $m/z=42$  ( $\text{C}_3\text{H}_6$ ),  $m/z=44$  ( $\text{CO}_2$ ),  $m/z=56$  ( $\text{C}_4\text{H}_8$ ) and  $m/z=58$  (acetone). The MS signals were calibrated for each channel and corrected for cracking contributions from different components.

#### Ethylene/2-Butene Titration and Ethylene-TPSR-MS.

The  $\text{C}_2\text{H}_4/2\text{-C}_4\text{H}_8$ -Titration and subsequent  $\text{C}_2\text{H}_4$ -TPSR-MS experiments were also performed with the Altamira Instruments AMI-200. The dehydration procedure was the same as given above for the Raman studies. After dehydration, the catalysts were activated with 1%  $2\text{-C}_4\text{H}_8/\text{Ar}$  (Praxair, Purity 99%, 30 mL/min) at activation temperatures of  $450^\circ\text{C}$  ( $\text{ReO}_x/\text{SiO}_2$ ),  $550^\circ\text{C}$  ( $\text{MoO}_x/\text{SiO}_2$ ), and  $650^\circ\text{C}$  ( $\text{WO}_x/\text{SiO}_2$ ) for 30 min. Different activation temperatures were employed because the catalysts activated at different temperatures. The reactor was then cooled to  $100^\circ\text{C}$  in flowing 1%  $2\text{-C}_4\text{H}_8/\text{Ar}$  (Praxair, Purity 99%, 30 mL/min), and the temperature was then held at  $100^\circ\text{C}$  for 30 min in flowing 1%  $\text{C}_2\text{H}_4/\text{Ar}$  (Praxair, Purity 99%, 30 mL/min). Subsequently, the temperature was ramped at  $10^\circ\text{C}/\text{min}$  to  $600^\circ\text{C}$  for  $\text{ReO}_x/\text{MoO}_x$  and  $800^\circ\text{C}$  for  $\text{WO}_x$  catalysts to titrate the surface intermediates generated from 2-butene chemisorption after the high temperature activation. Only one surface  $\text{Re}=\text{CHCH}_3/\text{Mo}=\text{CHCH}_3/\text{W}=\text{CHCH}_3$  intermediates was assumed to be present on the  $\text{SiO}_2$ -supported  $\text{ReO}_x/\text{MoO}_x/\text{WO}_x$  catalysts, respectively, after saturation of the surface with 2-butene at  $100^\circ\text{C}$ . The number of activated surface sites was assumed to be equal to the number of  $\text{C}_3\text{H}_6$  molecules produced during subsequent  $\text{C}_2\text{H}_4\text{-C}_4\text{H}_8$  titration with the  $\text{C}_2\text{H}_4$ -TPSR-MS experiment. The same  $m/z$  channels were monitored as for the above  $2^{\text{nd}}$   $\text{C}_3\text{H}_6$ -TPSR-MS experiments.

#### Steady State Propylene Metathesis.

The steady state propylene self-metathesis activities were also measured in the Altamira Instruments AMI-200. The dehydration procedure was the same as indicated above for the Raman experiments. After dehydration, the catalysts were activated with 5%  $\text{C}_3\text{H}_6/\text{Ar}$  (Praxair, Purity 99%, 30 mL/min) at the activation temperatures of  $450^\circ\text{C}$  ( $\text{ReO}_x/\text{SiO}_2$ ),  $550^\circ\text{C}$  ( $\text{MoO}_x/\text{SiO}_2$ ), and  $650^\circ\text{C}$  ( $\text{WO}_x/\text{SiO}_2$ ) for 30 min. The reactor temperature was then changed to various steady state reaction temperatures from  $100^\circ\text{C}$  up to  $550^\circ\text{C}$  in flowing Ar (Air Gas, UHP, 30 mL/min). Note that each catalyst required a different activation and reaction temperature because of the different stability or reducibility of the surface  $\text{MO}_x$  sites on  $\text{SiO}_2$ . The steady state reaction was performed by flowing 5%  $\text{C}_3\text{H}_6/\text{Ar}$  (Praxair, Purity 99%, 30 mL/min) at the reaction temperatures for 60 min. The catalytic activities (mmol/g/h) were obtained by normalizing the conversion of propylene by

the flow rate and catalyst weight. The turnover frequency (TOF) values were obtained by normalizing the steady state activity by the number of activated surface sites determined from the  $\text{C}_2\text{H}_4/\text{C}_4\text{H}_8$  titration.

### III. Results

#### *In situ* DRIFTS of Surface Hydroxyl Anchoring Sites.

The *in situ* DRIFTS difference spectra of the  $\text{SiO}_2$ -supported metal oxide catalysts under dehydrated conditions are presented in Figure 1. The bare  $\text{SiO}_2$  support contains both isolated  $\text{Si}-\text{OH}$  ( $3737\text{ cm}^{-1}$ ) and geminal  $\text{Si}(\text{-OH})_2$  (broad peak  $\sim 3727\text{--}3755\text{ cm}^{-1}$ ) surface hydroxyls. The difference spectra between the supported  $\text{MO}_x/\text{SiO}_2$  catalysts and the  $\text{SiO}_2$  support reveal that the supported  $\text{ReO}_x$ ,  $\text{MoO}_x$  and  $\text{WO}_x$  sites mainly anchored at the isolated  $\text{Si}-\text{OH}$  surface hydroxyls.<sup>6, 12-13</sup>

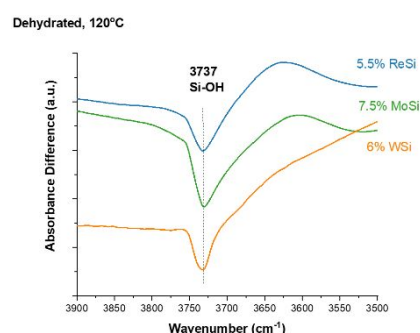


**Figure 1.** *In situ* DRIFTS difference spectra of the surface hydroxyl region of the  $\text{SiO}_2$ -supported catalysts metal oxide under dehydrated conditions ( $120^\circ\text{C}$ ). The spectrum of the dehydrated  $\text{SiO}_2$  support was subtracted from the spectrum of each  $\text{SiO}_2$ -supported metal oxide catalyst.

#### *In situ* Raman under dehydrated, activated and re-oxidized conditions.

**Dehydrated Conditions.** The *in situ* Raman spectra of the  $\text{SiO}_2$ -supported metal oxide catalysts under dehydrated, activated and re-oxidized conditions are presented in Figure 2 with the assignments of the vibrational bands. The  $\text{SiO}_2$  support gives rise to Raman bands  $\sim 500$ ,  $607$ ,  $800\text{ cm}^{-1}$ , along with a weak band  $\sim 970\text{ cm}^{-1}$  from the surface  $\text{Si}-\text{OH}$  vibration that is overshadowed by the strong  $\text{Mo}=\text{O}$  and  $\text{W}=\text{O}$  bands of the surface metal oxides.<sup>12,14</sup> The absence of strong Raman bands from crystalline  $\text{Re}_2\text{O}_7$  ( $798$ ,  $820$ ,  $993\text{ cm}^{-1}$ ),  $\text{MoO}_3$  ( $820$ ,  $997\text{ cm}^{-1}$ ) and  $\text{WO}_3$  ( $715$ ,  $806\text{ cm}^{-1}$ ) indicate that the surface coverage of  $\text{ReO}_x$ ,  $\text{MoO}_x$  and  $\text{WO}_x$  sites are maximized without formation of crystalline  $\text{Re}_2\text{O}_7$ ,  $\text{MoO}_3$  and  $\text{WO}_3$  nanoparticles on the  $\text{SiO}_2$  support.<sup>12</sup> Furthermore, the absence of bridging  $\text{Re}-\text{O}-\text{Re}$ ,  $\text{Mo}-\text{O}-\text{Mo}$  and  $\text{W}-\text{O}-\text{W}$  Raman bands at  $\sim 200\text{--}300\text{ cm}^{-1}$  indicates that these surface metal oxides are present as isolated sites, which is also confirmed with UV-vis.<sup>6,12-13,15</sup> The surface  $\text{ReO}_x$  sites have a strong  $\nu_s(\text{Re}=\text{O})$  band at  $1012\text{ cm}^{-1}$  and a relatively weak  $\nu_{as}(\text{Re}=\text{O})$  band at  $987\text{ cm}^{-1}$  from tri-oxo  $(\text{O}=\text{O})_3\text{Re}-\text{O}-\text{Si}$  sites.<sup>6,15</sup> The surface  $\text{MoO}_x$  sites exhibit a strong  $\nu_s(\text{Mo}=\text{O})$  band at  $986\text{ cm}^{-1}$  and a relatively weak  $\nu_{as}(\text{Mo}=\text{O})$  band at  $964\text{ cm}^{-1}$  from surface dioxo  $(\text{O}=\text{O})_2\text{Mo}(\text{-O-Si})_2$  sites.<sup>13,15</sup> The surface  $\text{WO}_x$  sites possess a strong  $\nu_s(\text{W}=\text{O})$  band at  $980$

$\text{cm}^{-1}$  from di-oxo ( $\text{O}=\text{O}$ ) $_2\text{W}-\text{O}_2$  sites and a relatively weak  $\nu_s(\text{W}=\text{O})$  band at  $1008\text{ cm}^{-1}$  from a minor amount of mono-oxo  $\text{O}=\text{W}(-\text{O}-\text{Si})_4$  sites.<sup>12,15</sup>

**Activation and Re-oxidation Conditions.** The prior dehydration, activation and re-oxidation temperatures were determined from the 1<sup>st</sup>  $\text{C}_3\text{H}_6$ -TPSR-MS findings given below. The *in situ* Raman spectra of  $\text{SiO}_2$  supported metal oxide catalysts under activation and re-oxidation conditions are shown in Figure 2 and S1. After 90 min of  $\text{C}_3\text{H}_6$  activation at high temperatures, the intensity of the Raman bands of all the  $\text{SiO}_2$ -supported metal oxide catalysts significantly diminished primarily due to the accumulation of coke on the surface, blocking the detection of surface metal oxide sites. After re-oxidation with  $\text{O}_2$  for 60 min, the surface coke was burned off and the activated surface  $\text{ReO}_x$ ,  $\text{MoO}_x$  and  $\text{WO}_x$  sites that only represent a smaller portion of total surface metal oxide sites were successfully re-oxidized back to their dehydrated state. The Raman bands of  $\nu_s(\text{Re}=\text{O})$  and  $\nu_{as}(\text{Re}=\text{O})$  from the surface  $\text{ReO}_x$  sites and  $\nu_s(\text{Mo}=\text{O})$  and  $\nu_{as}(\text{Mo}=\text{O})$  bands from the surface  $\text{MoO}_x$  sites exhibit notably lower Raman band intensities compared to the band intensities after the initial dehydration. The approximate decrease in the area of the Raman bands relative to the  $\text{SiO}_2$  support band at  $\sim 607\text{ cm}^{-1}$  follows the trend:  $\text{ReO}_x$  ( $\sim 49\%$ ) >  $\text{MoO}_x$  ( $\sim 38\%$ ) >>  $\text{WO}_x$  ( $\sim 4\%$ ). The reduction in intensity of the Raman bands indicates the significant loss of surface  $\text{ReO}_x$ <sup>16</sup> and  $\text{MoO}_x$ <sup>17</sup> sites from these catalysts due to their volatility at high temperatures. The intensity of the Raman band of the  $\nu_s(\text{W}=\text{O})$  of surface  $\text{WO}_x$  sites, however, was almost fully recovered to that of the initial dehydration treatment, reflecting minimal volatilization of  $\text{WO}_x$  at elevated temperatures.

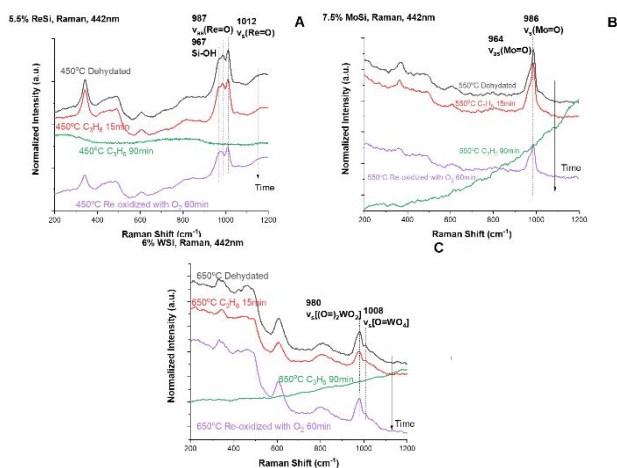


**Figure 2.** *In situ* Raman spectra ( $200\text{--}1200\text{ cm}^{-1}$ ) of the  $\text{SiO}_2$ -supported metal oxide catalysts after dehydration, propylene activation and re-oxidation conditions: (A)  $\text{ReO}_x/\text{SiO}_2$  at  $450\text{ }^\circ\text{C}$ , (B)  $\text{MoO}_x/\text{SiO}_2$  at  $550\text{ }^\circ\text{C}$  and (C)  $\text{WO}_x/\text{SiO}_2$  at  $650\text{ }^\circ\text{C}$ .

### $\text{C}_3\text{H}_6$ -TPSR-MS.

**1<sup>st</sup>  $\text{C}_3\text{H}_6$ -TPSR-MS cycle.** The 1<sup>st</sup>  $\text{C}_3\text{H}_6$ -TPSR-MS spectra of the dehydrated  $\text{SiO}_2$  supported metal oxide catalysts are

presented in Figure 3. The dehydrated supported  $\text{ReO}_x/\text{SiO}_2$  catalyst only produces  $\text{C}_4\text{H}_8$  at the high temperatures of  $\sim 420\text{--}550\text{ }^\circ\text{C}$  ( $T_p=450\text{ }^\circ\text{C}$ ). Similarly, the dehydrated supported  $\text{MoO}_x/\text{SiO}_2$  catalyst only produces  $\text{C}_4\text{H}_8$  at somewhat higher temperatures of  $\sim 350\text{--}600\text{ }^\circ\text{C}$  ( $T_p=520\text{ }^\circ\text{C}$ ). The dehydrated supported  $\text{WO}_x/\text{SiO}_2$  catalyst only produces  $\text{C}_4\text{H}_8$  at even higher temperatures of  $\sim 550\text{--}785\text{ }^\circ\text{C}$  ( $T_p=718\text{ }^\circ\text{C}$ ). All the  $\text{SiO}_2$ -supported metal oxide catalysts also produce oxygenated products ( $\text{CO}$ ,  $\text{CO}_2$ , and  $\text{H}_2\text{O}$ ) at high temperatures from partial reduction of surface metal oxide sites by propylene during the catalyst activation stage. While the combustion products precede the formation of butene for the supported  $\text{ReO}_x/\text{SiO}_2$  catalyst, the combustion products primarily form after the start of butene formation for the supported  $\text{MoO}_x/\text{SiO}_2$  and  $\text{WO}_x/\text{SiO}_2$  catalysts. The supported  $\text{WO}_x/\text{SiO}_2$  catalyst has relatively higher  $\text{CO}/\text{CO}_2$  production ratio than the supported  $\text{ReO}_x/\text{SiO}_2$  and  $\text{MoO}_x/\text{SiO}_2$  catalysts. The propylene metathesis activation product acetone is only observed from the supported  $\text{ReO}_x/\text{SiO}_2$  ( $T_p=133$ ,  $412\text{ }^\circ\text{C}$ ) and  $\text{MoO}_x/\text{SiO}_2$  ( $T_p=190$ ,  $520\text{ }^\circ\text{C}$ ) catalysts. It is possible that acetone decomposed at the much higher temperatures required for activation of the surface  $\text{WO}_x$  sites on  $\text{SiO}_2$  or that a different activation path is followed by the supported  $\text{WO}_x/\text{SiO}_2$  catalyst.

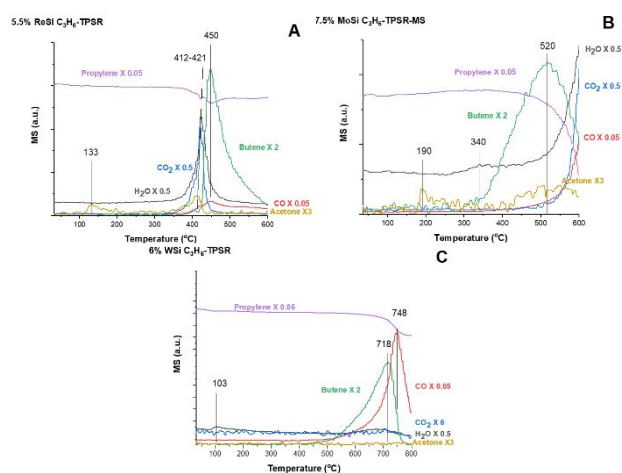


**Figure 3.** The 1<sup>st</sup>  $\text{C}_3\text{H}_6$ -TPSR-MS cycle spectra ( $30\text{--}600/800\text{ }^\circ\text{C}$ ) of the  $\text{SiO}_2$ -supported metal oxide catalysts: (A)  $\text{ReO}_x/\text{SiO}_2$ , (B)  $\text{MoO}_x/\text{SiO}_2$ , and (C)  $\text{WO}_x/\text{SiO}_2$ .

**2<sup>nd</sup>  $\text{C}_3\text{H}_6$ -TPSR-MS cycle.** The 2<sup>nd</sup>  $\text{C}_3\text{H}_6$ -TPSR-MS spectra of  $\text{SiO}_2$ -supported metal oxide catalysts that have been activated by the 1<sup>st</sup>  $\text{C}_3\text{H}_6$ -TPSR cycle are presented in Figure 4, and allows chemically probing the properties of the activated sites in the 1<sup>st</sup>  $\text{C}_3\text{H}_6$ -TPSR cycle. The activated supported  $\text{ReO}_x/\text{SiO}_2$  catalyst produces  $\text{C}_4\text{H}_8$  at intermediate temperatures  $\sim 250\text{--}400\text{ }^\circ\text{C}$  ( $T_p=300\text{ }^\circ\text{C}$ ) and high temperatures  $\sim 420\text{--}550\text{ }^\circ\text{C}$  ( $T_p=470\text{ }^\circ\text{C}$ ), but the amount of  $\text{C}_4\text{H}_8$  produced is drastically decreased compared to the 1<sup>st</sup> cycle. The activated supported  $\text{MoO}_x/\text{SiO}_2$  catalyst produces  $\text{C}_4\text{H}_8$  at both low  $\sim 30\text{--}250\text{ }^\circ\text{C}$  ( $T_p=107\text{ }^\circ\text{C}$ ) and high temperatures  $\sim 250\text{--}600\text{ }^\circ\text{C}$  ( $T_p=470\text{ }^\circ\text{C}$ ) with a much larger



amount of  $C_4H_8$  produced compared to the 1<sup>st</sup> cycle. The activated supported  $WO_x/SiO_2$  catalyst produces  $C_4H_8$  at both low  $\sim 30$ – $170^\circ C$  ( $T_p=87^\circ C$ ) and high temperatures  $\sim 350$ – $800^\circ C$  ( $T_p=576^\circ C$ ) with a much larger amount of  $C_4H_8$  produced compared to the 1<sup>st</sup> cycle. The  $C_4H_8$  production during the 2<sup>nd</sup>  $C_3H_6$ -TPSR cycle follows the trend (i) at low temperatures:  $MoO_x > WO_x \gg ReO_x$ , and (ii) at high temperatures  $WO_x > MoO_x \gg ReO_x$ . The consumption of  $C_3H_6$  during the 2<sup>nd</sup>  $C_3H_6$ -TPSR cycle is compared in Figure S2. The activated supported  $MoO_x/SiO_2$  and  $WO_x/SiO_2$  catalysts consume propylene for  $C_3H_6$  self-metathesis at low temperature and consume propylene for both  $C_3H_6$  self-metathesis and  $C_3H_6$  combustion at high temperature. The activated supported  $ReO_x/SiO_2$  catalyst exhibits only minor  $C_3H_6$  consumption at both low and high temperatures.

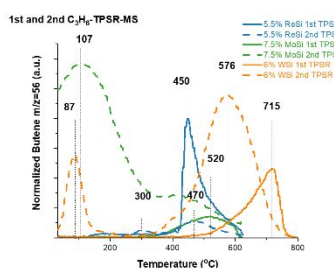


**Figure 4.** The  $C_4H_8$  production of 1<sup>st</sup> and 2<sup>nd</sup>  $C_3H_6$ -TPSR -MS (30–600/800  $^\circ C$ ) cycles with online MS for the  $SiO_2$  supported metal oxide catalysts. The MS signals of  $C_4H_8$  were normalized by the MS signals of the Ar carrier gas.

### $C_3H_6$ -TPSR-IR.

The *in situ*  $C_3H_6$ -TPSR-IR spectra of the dehydrated  $SiO_2$  supported metal oxide catalysts are presented in Figure S3. There is no notable difference between the 1<sup>st</sup> and 2<sup>nd</sup> cycle *in situ*  $C_3H_6$ -TPSR-IR spectra. For all the  $SiO_2$  supported metal oxide catalysts, the *in situ* IR spectra at  $30^\circ C$  are primarily composed of gas phase propylene (The *in situ* IR bands at  $\sim 1444$ ,  $1455$ ,  $1472$ ,  $1638$ , and  $1664\text{ cm}^{-1}$  correspond to gas phase propylene<sup>18</sup>). No detectable  $\nu(C=O)$  vibration at  $1686\text{ cm}^{-1}$  of surface acetone is observed on the  $SiO_2$ -supported metal oxide catalysts. Above  $320^\circ C$ , there are no IR bands of gas phase propylene and surface intermediates, reflecting thermal broadening of the gas phase bands and an extremely low density of surface intermediates, respectively. The broad *in situ* IR bands at  $\sim 1279$  and  $\sim 1570\text{ cm}^{-1}$  for  $SiO_2$ -supported metal oxide catalysts result from a thermal effect on the spectral baseline, and not from surface intermediates.<sup>13</sup>

### Ethylene/2-Butene Titration.

The  $C_2H_4/2-C_4H_8$  titration measurements were performed by activating the catalyst with  $2-C_4H_8$  at elevated temperatures, titrating the resulting surface  $M=CHCH_3$  intermediates with flowing  $C_2H_4$ -TPSR and quantifying the number of  $C_3H_6$  molecules produced with the online MS as shown in Figure S4. The initial  $C_2H_4/2-C_4H_8$  titration studies at  $100^\circ C$  (Figure S4 A), reveal that much more surface  $MoO_x$  sites were activated than

surface  $ReO_x$  and  $WO_x$  sites at  $100^\circ C$ . The  $C_2H_4$ -TPSR-MS spectra for the supported  $MO_x/SiO_2$  catalysts are presented in Figure S4 B and the corresponding number of activated sites are given in Table 1. The 2-butene activated supported  $ReO_x/SiO_2$  catalyst has only one  $C_3H_6$ -TPSR peak at  $505^\circ C$ , which represents activation of 17.1% of the total surface  $ReO_x$  sites. The 2-butene activated supported  $MoO_x/SiO_2$  catalyst exhibits two  $C_3H_6$ -TPSR peaks at  $100^\circ C$  and  $540^\circ C$  that represent 20.0% ( $100^\circ C$ ) and 1.1% ( $540^\circ C$ ) of activated surface  $MoO_x$  sites, respectively. Since a portion of the surface  $ReO_x$  and  $MoO_x$  sites volatilize during the high temperature  $C_3H_6$  activation, the actual fraction of activated surface  $ReO_x$  and  $MoO_x$  sites will be higher than the fractions indicated in Table 1. The 2-butene activated supported  $WO_x/SiO_2$  catalyst shows only one  $C_3H_6$ -TPSR peak at  $703^\circ C$  that represents 2.1% of activated surface  $WO_x$  sites. Although the supported  $ReO_x/SiO_2$  and  $MoO_x/SiO_2$  catalysts have a higher number of activated sites ( $\sim 20\%$  of the initial oxidized sites), the supported  $WO_x/SiO_2$  catalyst has an order of magnitude lower number of activated sites ( $\sim 2\%$  of the initial oxidized sites). Furthermore, since only surface  $MoO_x$  sites exhibit a  $C_3H_6$ -TPSR peak at low temperatures ( $\sim 100^\circ C$ ), this indicates that the surface  $Mo=CHCH_3$  intermediates are much more reactive at low temperatures than the surface  $Re=CHCH_3$  and  $W=CHCH_3$  intermediates towards ethylene titration.

Catalyst (wt.%)	Total Number of Initial Surface $MO_x$ Sites (mol)	Number of $C_3H_6$ Produced (mol)	Fraction of Activated surface Sites
5.5%ReSi	$2.3 \times 10^{-5}$	$3.9 \times 10^{-6}$ ( $505^\circ C$ )	17% ( $505^\circ C$ )
7.5%MoSi	$3.1 \times 10^{-5}$	$6.2 \times 10^{-6}$ ( $100^\circ C$ )	20% ( $100^\circ C$ )
		$3.5 \times 10^{-7}$ ( $540^\circ C$ )	1.1% ( $540^\circ C$ )
6%WSi	$2.5 \times 10^{-5}$	$5.3 \times 10^{-7}$ ( $703^\circ C$ )	2.1% ( $703^\circ C$ )

**Table 1.** Number of activated surface  $MO_x$  sites calculated from activation by 2- $C_4H_8$  and subsequent titration with  $C_2H_4$ -TPSR-MS. Fraction of activated sites referenced against total number of initial oxidized sites.

### Steady State Propylene Metathesis of catalysts activated with $C_3H_6$ .

The steady state propylene self-metathesis activity (mmol/g/h) and TOF ( $s^{-1}$ ) values of the activated  $SiO_2$ -supported metal oxide catalysts are presented in Table 2 as a function of reaction temperature and activation temperatures. At the reaction temperature of  $100^\circ C$ , the supported  $MoO_x/SiO_2$  catalyst is the most active catalyst while the supported  $ReO_x/SiO_2$  and  $WO_x/SiO_2$  catalysts are two-orders of magnitude less active. Increasing the reaction temperature decreases the activity of the supported  $MoO_x/SiO_2$  catalyst and increases the activity of the supported  $ReO_x/SiO_2$  and  $WO_x/SiO_2$  catalysts. Surprisingly, the activity of the supported  $MoO_x/SiO_2$  catalyst increases somewhat at a reaction temperature of  $550^\circ C$ . At the highest reaction temperature of

450-550°C, the supported  $\text{WO}_x/\text{SiO}_2$  catalyst is about an order of magnitude more active than the supported  $\text{MoO}_x/\text{SiO}_2$  and  $\text{ReO}_x/\text{SiO}_2$  catalysts. The corresponding TOF values follow the same trends as the activity values and reveal low specific reaction rates for olefin metathesis over this set of catalysts. At 100°C, the supported  $\text{MoO}_x/\text{SiO}_2$  has the highest TOF that is one to two orders of magnitude greater than the supported  $\text{ReO}_x/\text{SiO}_2$  and  $\text{WO}_x/\text{SiO}_2$  catalysts. At 550°C, the supported  $\text{WO}_x/\text{SiO}_2$  catalyst exhibits the highest TOF value that is about two orders of magnitude greater than that of the supported  $\text{MoO}_x/\text{SiO}_2$  and  $\text{ReO}_x/\text{SiO}_2$  catalysts. These olefin metathesis  $\text{SiO}_2$ -supported metal oxide catalysts exhibit a wide range of activity and TOF values that reveal different dependence on the reaction temperature with the supported  $\text{MoO}_x/\text{SiO}_2$  catalyst most active at lower temperatures and supported  $\text{WO}_x/\text{SiO}_2$  catalyst most active at high temperatures.

surface coverage is well above the maximum dispersion limit on  $\text{SiO}_2$  or monolayer coverage.<sup>12</sup> The dehydrated surface  $\text{ReO}_x$  sites are present as fully oxidized  $\text{Re}(+7)$  cations with an isolated tri-oxo  $(\text{O})_3\text{ReO}$  structure.<sup>6,15</sup> The dehydrated surface  $\text{MoO}_x$  sites are present as fully oxidized  $\text{Mo}(+6)$  cations as isolated di-oxo  $(\text{O})_2\text{MoO}_2$  sites.<sup>13,15</sup> The surface dehydrated  $\text{WO}_x$  sites are present as fully oxidized  $\text{W}(+6)$  with a mixture of isolated di-oxo  $(\text{O})_2\text{WO}_2$  and a small amount of mono-oxo  $(\text{O})\text{WO}_4$  sites.<sup>15,21</sup> These surface isolated  $\text{MO}_x$  structures are in agreement with the structures reported in the literature for dehydrated supported  $\text{MO}_x/\text{SiO}_2$  catalysts from multiple *in situ* characterization studies (Raman,<sup>12, 15, 22-24</sup> UV-vis,<sup>22-23</sup> IR,<sup>22</sup> and XAS<sup>22,24</sup>) and DFT calculations<sup>25-27</sup>. The nature of the activated surface  $\text{MO}_x$  sites on  $\text{SiO}_2$ , however, still require direct spectroscopic characterization because the activated surface  $\text{MO}_x$  sites possess the same oxidation state as the unactivated sites, which complicates the spectroscopic deconvolution of the unactivated and activated sites. The presence of carbon deposits (coke) on the catalysts also adds additional complexity to the analysis. The initial formation of surface metal=carbene proceeds via a mechanism where the fully oxidized surface metal-oxo sites ( $\text{Re}(\text{O})_3$ ,  $\text{O}=\text{Mo}=\text{O}$ ,  $\text{O}=\text{W}=\text{O}$ ,  $\text{W}=\text{O}$ ) initially reduce to a lower oxidation state by the olefins as the oxo-oxygen is removed and then re-oxidized back to the highest oxidation state via formation of surface  $\text{M}=\text{CH}_2$  and  $\text{M}=\text{CHCH}_3$  species.<sup>25</sup> The  $\text{C}_2\text{H}_4/2\text{-C}_4\text{H}_8$  titration studies clearly demonstrate that surface  $\text{M}=\text{CHCH}_3$  and  $\text{M}=\text{CH}_2$  intermediates are indeed present on the activated catalysts.

#### Volatilization of surface $\text{MO}_x$ sites from the $\text{SiO}_2$ support during activation

Volatilization of the active component in heterogeneous catalysts is a serious concern since it leads to loss of expensive catalyst components as well as catalyst deactivation (fewer catalytic active sites). The current study demonstrated that an appreciable fraction of surface  $\text{ReO}_x$  (~49%) and  $\text{MoO}_x$  (~38%) sites on  $\text{SiO}_2$  volatilizes during the high temperature  $\text{C}_3\text{H}_6$  activation, which is a required step for activation of active olefin metathesis catalysts.<sup>2, 8</sup> In contrast, only a negligible fraction of surface  $\text{WO}_x$  sites (~4%) on  $\text{SiO}_2$  volatilizes (Figure 2). Additional surface  $\text{ReO}_x$  and  $\text{MoO}_x$  sites probably volatilize under olefin metathesis reaction conditions at high temperatures and catalyst regeneration under oxidizing conditions that are required to remove catalyst coke, especially at elevated temperatures. Volatilization of surface  $\text{MO}_x$  sites on  $\text{SiO}_2$  takes place by hydrolysis of bridging  $\text{M}-\text{O}-\text{Si}$  bonds that forms  $\text{M}-\text{OH}$  and  $\text{HO}-\text{Si}$ , which weakens the metal oxide-silica interaction.<sup>28, 29</sup> The extent of volatilization is related to the lower sublimation temperatures of  $\text{Re}_2\text{O}_7$  (~250°C)<sup>16</sup> and  $\text{MoO}_3$  (~525°C)<sup>17</sup> compared to  $\text{WO}_3$  (800°C)<sup>30</sup>. Thus, the supported  $\text{WO}_x/\text{SiO}_2$  catalyst is more robust in comparison to the supported  $\text{ReO}_x/\text{SiO}_2$  and  $\text{MoO}_x/\text{SiO}_2$  catalysts for olefin metathesis, especially under harsh elevated temperatures. It is important to note that the initial number of surface  $\text{MO}_x$  sites on the  $\text{SiO}_2$  support is not a critical parameter since the number of stable surface  $\text{MO}_x$  sites is

Catalyst (Activation Temperature)	Steady State Activity (mmol/g/h) (TOF (s <sup>-1</sup> ))* *TOF normalized by number of sites determined with $\text{C}_2\text{H}_4/\text{C}_4\text{H}_8$ titration				
	100°C	200°C	300°C	400°C	450°C or 550°C
5.5%ReSi (450°C)	0.03 (0.22x10 <sup>-3</sup> )	0.03 (0.22x10 <sup>-3</sup> )	0.10 (0.73x10 <sup>-3</sup> )	0.38 (2.80x10 <sup>-3</sup> )	0.51 (450°C) (3.70x10 <sup>-3</sup> )
7.5%MoSi (550°C)	4.0 (1.7x10 <sup>-2</sup> )	2.0 (0.85x10 <sup>-2</sup> )	0.03 (0.13x10 <sup>-3</sup> )	0.01 (0.43x10 <sup>-4</sup> )	0.48 (550°C) (0.20x10 <sup>-2</sup> )
6%WSi (650°C)	0.02 (0.11x10 <sup>-2</sup> )	0.03 (0.16x10 <sup>-2</sup> )	0.03 (0.16x10 <sup>-2</sup> )	0.23 (0.12x10 <sup>-1</sup> )	3.6 (550°C) (1.9x10 <sup>-1</sup> )

**Table 2.** Steady state activity (mmol/g/h) and TOF values of  $\text{C}_3\text{H}_6$  pre-activated catalysts (catalyst activation temperatures are indicated in Table 2).

## IV. Discussion

### Anchoring of $\text{MO}_x$ Species on $\text{SiO}_2$ Surface Hydroxyls

The metal oxides preferentially anchor at the isolated  $\text{Si}-\text{OH}$  surface hydroxyls. The geminal  $\text{Si}(\text{OH})_2$  surface hydroxyls are either unreactive or minimally reactive towards anchoring of the aqueous  $\text{ReO}_x$ ,  $\text{MoO}_x$  and  $\text{WO}_x$  species (Figure 1). Consequently, all three metal oxides primarily anchor at the same isolated silanol  $\text{Si}-\text{OH}$  surface hydroxyls.<sup>19-20</sup>

### Molecular and Electronic Structure of Surface $\text{ReO}_x$ , $\text{MoO}_x$ , $\text{WO}_x$ sites on $\text{SiO}_2$ under oxidative dehydration and olefin activation conditions.

The initial dehydrated surface  $\text{MO}_x$  sites on  $\text{SiO}_2$  are completely dispersed as isolated sites on the  $\text{SiO}_2$  support. The presence of only isolated surface metal oxide sites on  $\text{SiO}_2$  supports is related to the low density of reactive surface hydroxyl anchoring sites associated with the isolated  $\text{Si}-\text{OH}$  surface hydroxyls. Crystalline  $\text{Re}_2\text{O}_7$ ,  $\text{MoO}_3$ , and  $\text{WO}_3$  nanoparticles are not present and are only present when the

controlled by metal oxide volatilization during catalyst activation and the olefin metathesis reaction.

#### Number of Activated Surface $\text{MO}_x$ Sites on $\text{SiO}_2$

Although both surface  $\text{MoO}_x$  and  $\text{WO}_x$  on  $\text{SiO}_2$  predominantly possess the same initial dioxo surface  $(\text{O}=\text{O})_2\text{M}(\text{O})_2$  sites, they have very different responses towards activation by the ethylene/2-butene titration. A higher fraction ( $\sim 20\%$ ) of the surface  $\text{Mo}=\text{CHCH}_3$  intermediates undergo metathesis with  $\text{C}_2\text{H}_4$  at low temperatures to yield  $\text{C}_3\text{H}_6$ . In contrast, only a minor fraction of the surface  $\text{W}=\text{CHCH}_3$  intermediates undergo metathesis with  $\text{C}_2\text{H}_4$  and require high temperatures to yield  $\text{C}_3\text{H}_6$ . This difference in fraction of activated sites between  $\text{MoO}_x/\text{SiO}_2$  and  $\text{WO}_x/\text{SiO}_2$  catalysts is related to the more facile reduction by propylene of surface  $\text{MoO}_4$  sites on  $\text{SiO}_2$  than the surface  $\text{WO}_4$  sites on  $\text{SiO}_2$  ( $\text{Mo}$  ( $T_p = 520^\circ\text{C}$ ) and  $\text{W}$  ( $T_p = 715^\circ\text{C}$ ). The fraction of activated sites in  $\text{MoO}_x/\text{SiO}_2$  and  $\text{WO}_x/\text{SiO}_2$  catalysts are limited by the suitable geometry and neighborhood of surface sites that can be effectively activated by alkenes.<sup>26</sup> The trioxo surface  $(\text{O}=\text{O})_3\text{Re}(\text{O})$  sites possess a different structure than the surface  $\text{MoO}_4$  and  $\text{WO}_4$  sites, but responds similarly to the surface  $\text{MoO}_4$  sites with  $\sim 17\%$  of the surface  $\text{ReO}_4$  sites becoming activated by exposure to propylene ( $T_p = 450^\circ\text{C}$ ). The facile reduction by propylene of the surface  $\text{ReO}_4$  sites is related to rhenia's intrinsic ease of reduction.<sup>7</sup>

#### Activation of $\text{SiO}_2$ -supported $\text{MO}_x$ catalysts by $\text{C}_3\text{H}_6$

The lower activation temperature of the supported  $\text{MoO}_x/\text{SiO}_2$  catalyst than the supported  $\text{WO}_x/\text{SiO}_2$  catalyst is agreement with the DFT calculation that reveals lower predicted overall activation Gibbs energies for the  $\text{MoO}_x/\text{SiO}_2$  than the  $\text{WO}_x/\text{SiO}_2$  catalyst.<sup>31</sup> The 1<sup>st</sup>  $\text{C}_3\text{H}_6$ -TPSR indicates the temperatures where each of the surface  $\text{MO}_x$  sites on  $\text{SiO}_2$  become activated, while the 2<sup>nd</sup>  $\text{C}_3\text{H}_6$ -TPSR reveals the reactivity of the activated surface  $\text{MO}_x$  sites. Both supported  $\text{MoO}_x/\text{SiO}_2$  and  $\text{WO}_x/\text{SiO}_2$  catalysts reveal the presence of highly active surface  $\text{MO}_x$  sites on  $\text{SiO}_2$  at  $\sim 100^\circ\text{C}$  after high temperature activation ( $>400^\circ\text{C}$ ). For supported  $\text{MoO}_x/\text{SiO}_2$ , however, most of the activated sites perform olefin metathesis at  $\sim 100^\circ\text{C}$  while most of the activated sites for supported  $\text{WO}_x/\text{SiO}_2$  perform olefin metathesis at  $\sim 600^\circ\text{C}$ . This difference in activity is reflected in the olefin metathesis reaction rates of these two supported  $\text{MO}_x/\text{SiO}_2$  catalysts, which will be elaborated upon below. The activated surface  $\text{ReO}_x$  sites on  $\text{SiO}_2$  don't possess low temperature activated sites and only exhibit modest olefin metathesis activity at intermediate reaction temperatures ( $\sim 470^\circ\text{C}$ ).

#### Activity and TOF of $\text{SiO}_2$ -supported $\text{MO}_x$ catalysts for propylene metathesis.

The steady state activity (mmol/g/h) of the catalysts, which doesn't take into account the number of volatilized  $\text{MoO}_x$  sites, indicates that the supported  $\text{MoO}_x/\text{SiO}_2$  and  $\text{WO}_x/\text{SiO}_2$  catalysts are the most active for propylene metathesis. However, the supported  $\text{MoO}_x/\text{SiO}_2$  is most active at low temperatures ( $100^\circ\text{C}$ ) while supported  $\text{WO}_x/\text{SiO}_2$  is most active

at high temperatures ( $550^\circ\text{C}$ ). It appears that the steady state olefin metathesis activity is dominated by the abundant number of low temperature active surface  $\text{MoO}_x$  sites for  $\text{MoO}_x/\text{SiO}_2$  while the steady state olefin metathesis activity is dominated by the abundant number of high temperature activated surface  $\text{WO}_x$  sites for  $\text{WO}_x/\text{SiO}_2$ . This difference in low temperature metathesis activity is a direct consequence of the reactivity of the surface  $\text{M}=\text{CHCH}_3$  and  $\text{M}=\text{CH}_2$  intermediates ( $\text{Mo} \gg \text{W}$ ). This is further reflected in the specific reactivity (TOF) values where supported  $\text{MoO}_x/\text{SiO}_2$  exhibits a TOF values of  $1.7 \times 10^{-2}/\text{s}$  at  $100^\circ\text{C}$  and  $0.20 \times 10^{-2}/\text{s}$  at  $550^\circ\text{C}$ . The decreasing performance of the supported  $\text{MoO}_x/\text{SiO}_2$  catalyst with increasing temperatures may be related to additional volatilization of  $\text{MoO}_x$  during olefin metathesis or possibly coking of the catalyst since catalytic kinetics should increase with reaction temperature. The corresponding supported  $\text{WO}_x/\text{SiO}_2$  exhibits TOF values of  $0.11 \times 10^{-2}/\text{s}$  at  $100^\circ\text{C}$  and  $1.9 \times 10^{-1}/\text{s}$  at  $550^\circ\text{C}$ . In contrast to the activated supported  $\text{MoO}_x/\text{SiO}_2$  and  $\text{WO}_x/\text{SiO}_2$  catalysts, the supported  $\text{ReO}_x/\text{SiO}_2$  possesses much lower TOF values of  $0.22 \times 10^{-3}/\text{s}$  at  $100^\circ\text{C}$  and  $3.7 \times 10^{-3}/\text{s}$  at  $450^\circ\text{C}$ . Since the surface  $\text{MO}_x$  sites are isolated on the  $\text{SiO}_2$  support and almost exclusively anchored at the same surface silanol, the TOF values will be independent of surface  $\text{MO}_x$  coverage. Note that these TOF values are true TOF values that are only based on the remaining active sites titrated after activation and volatilization. At high temperatures, the surface  $\text{WO}_x$  sites possess the most active sites (highest TOF) compared to the surface  $\text{MoO}_x$  sites (TOF is  $\sim 10\times$  less active) and surface  $\text{ReO}_x$  sites (TOF is  $\sim 100\times$  less active). The differing activation temperatures and reaction temperatures for the supported  $\text{MO}_x/\text{SiO}_2$  catalysts are related to the stability of the surface  $\text{M}=\text{O}$  oxo and  $\text{M}=\text{Carbene}$  bonds, respectively.

## Conclusions

The side-by-side comparison of the  $\text{SiO}_2$ -supported  $\text{ReO}_x$ ,  $\text{MoO}_x$  and  $\text{WO}_x$  catalysts provides fundamental insights about the different characteristics of these supported  $\text{MO}_x/\text{SiO}_2$  catalysts for olefin metathesis. All three metal oxides selectively anchor at the isolated surface  $\text{Si}-\text{OH}$  silanols and are present as isolated sites. The surface  $\text{MoO}_x$  and  $\text{WO}_x$  on  $\text{SiO}_2$  essentially possess the same molecular structures (dioxo  $(\text{O}=\text{O})_2\text{MoO}_2$  and  $(\text{O}=\text{O})_2\text{WO}_2$ ) while the surface  $\text{ReO}_x$  on  $\text{SiO}_2$  is present as trioxo  $((\text{O}=\text{O})_3\text{ReO})$ . The different molecular structures are related to the greater number of bonding electrons in the surface  $\text{Re}^{7+}\text{O}_x$  site than the surface  $\text{Mo}^{6+}\text{O}_x$  and  $\text{W}^{6+}\text{O}_x$  sites. These surface  $\text{MO}_x$  sites on  $\text{SiO}_2$  require activation by olefins at elevated temperatures to become active for olefin metathesis. The activation process removes the initial  $\text{M}=\text{O}$  oxo bonds forming coordinative unsaturated sites that allow for olefin chemisorption as surface  $\text{M}=\text{CHCH}_3$  and  $\text{M}=\text{CH}_2$  intermediate species, which are confirmed by the titration studies. The high temperature activation process, however, also leads to volatilization of the surface  $\text{MO}_x$  sites from the  $\text{SiO}_2$  support ( $\text{ReO}_x$  ( $\sim 49\%$ )  $>$   $\text{MoO}_x$  ( $\sim 38\%$ )  $\gg$   $\text{WO}_x$  ( $\sim 4\%$ )).

In spite of the  $\text{MO}_x$  volatilization, about 20% of the surface  $\text{MO}_x$  sites become activated for olefin metathesis by the supported



MoO<sub>x</sub>/SiO<sub>2</sub> and ReO<sub>x</sub>/SiO<sub>2</sub> catalysts at lower temperatures. In contrast, only about 2% of the surface WO<sub>x</sub> sites become activated for olefin metathesis by the supported WO<sub>x</sub>/SiO<sub>2</sub> catalysts at high temperatures. The number of activated sites is related to the ease of reduction of the initial surface MO<sub>x</sub> sites on SiO<sub>2</sub>. The reactivity of the surface M=carbenes (M=CHCH<sub>3</sub>/M=CH<sub>2</sub>) for olefin metathesis also follows the same trend: Mo=carbene > Re=carbene > W=carbene. As a result, during the steady state metathesis the surface MoO<sub>x</sub> sites are active at lower temperatures (~100°C), the surface WO<sub>x</sub> sites are active at high temperatures (~600°C) and the surface ReO<sub>x</sub> sites are active at intermediate temperatures (~470°C). Consequently, the surface MoO<sub>x</sub> sites are the most active at lower temperatures (TOF= 1.7 × 10<sup>-2</sup>/s at 100°C), the surface ReO<sub>x</sub> sites are the least active at intermediate temperatures (TOF=3.7 × 10<sup>-3</sup>/s at 450°C) and the surface WO<sub>x</sub> sites are the most active at high temperatures (TOF=1.9 × 10<sup>-1</sup>/s at 550°C).

The superior performance of the commercial supported WO<sub>x</sub>/SiO<sub>2</sub> catalysts compared to the supported MoO<sub>x</sub>/SiO<sub>2</sub> and ReO<sub>x</sub>/SiO<sub>2</sub> catalysts is a consequence of its more robust properties: (i) much lower volatility, (ii) higher steady state activity at elevated temperatures, and (iii) higher TOF at elevated temperatures. In spite of the superior olefin metathesis performance by the supported WO<sub>x</sub>/SiO<sub>2</sub> catalyst, the supported WO<sub>x</sub>/SiO<sub>2</sub> catalyst suffers from (i) being more difficult to activate that requires much higher activation temperatures, and (ii) only forming a low number of activated sites. Nevertheless, the positive features significantly outweigh the negative features making the supported WO<sub>x</sub>/SiO<sub>2</sub> catalyst the superior catalyst for olefin metathesis of small olefins.

## Conflicts of interest

There are no conflicts to declare.

## Data availability

The data that support the findings of this study are available from the corresponding author upon reasonable request. The experimental data generated and analyzed during this study are included in this published article and its supplementary information files.

## Acknowledgements

This study was funded by the U.S. Department of Energy, Office of Science, Office of Basic Energy, Catalysis Science Program, under Award Number FG02-93ER14350.

## References

- (1) Ivin, K.J.; Mol, J.C. *Olefin Metathesis and Metathesis Polymerization*. Academic Press. 1997, London.
- (2) Mol, J. C. Industrial applications of olefin metathesis. *J. Mol. Catal. A: Chem.* 2004, 213, 39–45.
- (3) Tullo, A. H. Turning Ethylene into Propylene. *c&en.* 2007, 85, 17.
- (4) Lavrenov, A. V.; Saifulina, L. F.; Buluchevskii, E. A.; Bogdanets, E. N. Propylene Production Technology: Today and Tomorrow. *Catal. Ind.* 2015, 7 (3), 175–187.
- (5) Butler, J. R. Metathesis Catalyst for Olefin Production. US Patent, US20110077444 A1, 2011.
- (6) Zhang, B.; Wachs, I. E. Identifying the Catalytic Active Site for Propylene Metathesis by Supported ReO<sub>x</sub> Catalysts. *ACS Catal.*, 2021, 11, 1962–1976.
- (7) Vuurman, M. A.; Stufkens, D. J.; Oskam, A.; Wachs, I. E. Structural determination of surface rhenium oxide on various oxide supports (Al<sub>2</sub>O<sub>3</sub>, ZrO<sub>2</sub>, TiO<sub>2</sub> and SiO<sub>2</sub>). *J. Mol. Catal.* 1992, 76, 263–285.
- (8) Ding, K.; Gulec, A.; Johnson, A. M.; Drake, T. L.; Wu, W.; Lin, Y.; Weitz, E.; Marks, L. D.; Stair, P. C. Highly Efficient Activation, Regeneration, and Active Site Identification of Oxide-Based Olefin Metathesis Catalysts. *ACS Catal.* 2016, 6, 5740–5746.
- (9) Handzlik, J.; Ogonowski, J.; Stoch, J.; Mikolajczyk, M.; Michorczyk, P. Properties and metathesis activity of molybdena-alumina, molybdena-silica-alumina and molybdena-silica catalysts-a comparative study. *Appl. Catal. A: Gen.* 2006, 312, 213–219.
- (10) Lwin, S.; Wachs, I. E. Olefin Metathesis by Supported Metal Oxide Catalysts. *ACS Catal.* 2014, 4, 2505–2520.
- (11) Mol, J. C. Olefin metathesis over supported rhenium oxide catalysts. *Catal. Today.* 1999, 51, 289–299.
- (12) Lee, E. L.; Wachs, I. E. *In situ* Spectroscopic Investigation of the Molecular and Electronic Structures of SiO<sub>2</sub> Supported Surface Metal Oxides. *J. Phys. Chem. C.* 2007, 111, 14410–14425.
- (13) Zhang, B.; Ford, M. E.; Ream, E.; Wachs, I. E. Olefin metathesis over supported MoO<sub>x</sub> catalysts: influence of the oxide support. *Catal. Sci. Technol.*, 2023, 13, 217–225.
- (14) Zhang, B.; Lwin, S.; Xiang, S.; Frenkel, A. I.; Wachs, I. E. Tuning the Number of Active Sites and Turnover Frequencies by Surface Modification of Supported ReO<sub>4</sub>/(SiO<sub>2</sub>-Al<sub>2</sub>O<sub>3</sub>) Catalysts for Olefin Metathesis. *ACS Catal.* 2021, 11, 2412–2421.
- (15) Lee, E. L.; Wachs, I. E. *In Situ* Raman Spectroscopy of SiO<sub>2</sub>-Supported Transition Metal Oxide Catalysts: An Isotopic 18O–16O Exchange Study. *J. Phys. Chem. C* 2008, 112, 6487–6498.
- (16) Smith, W. T.; Line, L. E.; Bell, W. A. The Vapor Pressures of Rhenium Heptoxide and Perrhenic Acid. *J. Am. Chem. Soc.* 1952, 74, 4964.
- (17) Pampararo, G.; Garvarino, G.; Ardoino, N.; Riani, P.; Busca, G. A study of molybdena catalysts in ethanoxidation. Part 1. Unsupported and silica-supported MoO<sub>3</sub>. *J Chem Technol Biotechnol.* 2021, 96, 3293–3303.
- (18) Afeefy, H. Y.; Liebman, J. F.; Stein, S. E. Neutral Thermochemical Data. In *NIST Chemistry WebBook*; Linstrom, P. J., Mallard, W. G., Eds; NIST Standard Reference Database Number 69; National Institute of Standards and Technology: Gaithersburg, MD.
- (19) Knozinger, H.; Ratnasamy, P. Catalytic Aluminas: Surface Models and Characterization of Surface Sites. *Catal. Rev.: Sci. Eng.* 1978, 17, 31–37.
- (20) Burcham, L. J.; Datka, J.; Wachs, I. E. *In Situ* Vibrational Spectroscopy Studies of Supported Niobium Oxide Catalysts. *J. Phys. Chem. B.* 1999, 103, 6015–6024.
- (21) Liwn, S.; Li, Y.; Frenkel, A. I.; Wachs, I. E. Nature of WO<sub>x</sub> Sites on SiO<sub>2</sub> and Their Molecular Structure-Reactivity/Selectivity Relationships for Propylene Metathesis. *ACS Catal.* 2016, 6, 3061–3071.
- (22) Amakawa, K.; Sun, L.; Guo, C.; Havecker, M.; Kube, P.; Wachs, I. E.; Lwin, S.; Frenkel, I. E.; Patlolla, A.; Hermann, K.; Schlogl, R.; Trunschke, A. How Strain Affects the Reactivity of

Surface Metal Oxide Catalysts. *Angew. Chem. Int. Ed.* 2013, 52, 13553-13557.

(23) Tian, H.; Roberts, C.A.; Wachs, I.E., Molecular Structural Determination of Molybdena in Different Environments: Aqueous Solutions, Bulk Mixed Oxides, and Supported MoO<sub>3</sub> Catalysts. *J. Phys. Chem. C* 2010, 114, 14110–14120.

(24) Radhakrishnan, R.; Reed, C.; Oyama, S.T; Seman, M.; Kondo, J.N.; Domen, K.; Ohminami, Y.; Asakura, K. Variability in the Structure of Supported MoO<sub>3</sub> Catalysts: Studies Using Raman and X-ray Absorption Spectroscopy with ab Initio Calculations. *J. Phys. Chem. B* 2001, 105, 8519–8530.

(25) Handzlik, J.; Ogonowski, J. Structure of isolated molybdenum (VI) and molybdenum (IV) oxide species on silica: periodic and cluster DFT studies. *J. Phys. Chem. C* 2012, 116, 5571–5584.

(26) Handzlik, J.; Kurleto, K.; Gierada, M. Computational Insights into Active Site Formation during Alkene Metathesis over a MoO<sub>x</sub>/ SiO<sub>2</sub> Catalyst: The Role of Surface Silanols. *ACS Catal.* 2021, 11, 13575–13590.

(27) Chempath, S.; Zhang, Y.; Bell, A.T. DFT studies of the structure and vibrational spectra of isolated molybdena species supported on silica. *J. Phys. Chem. C* 2007, 111, 1291–1298.

(28) Howell, J. G.; Li, Y.; Bell, A. T. Propene Metathesis over Supported Tungsten Oxide Catalysts: A Study of Active Site Formation. *ACS Catal.* 2016, 6, 11, 7728-7738

(29) Le, A. V.; Rajbanshi, B.; Lobo, R. F.; Bai, P. Mechanistic study of heterogeneous propene metathesis on WO<sub>x</sub>/SiO<sub>2</sub> catalysts. *J. Catal.* 2023, 427, 115117

(30) Millner, T.; Neugebauer, J. Volatility of the Oxides of Tungsten and Molybdenum in the Presence of Water Vapour. *Nature*. 1949, 163, 601-602.

(31) Handzlik, J.; Gierada, M.; Kurleto, K. Role of Surface Silanols in Active Site Formation during Olefin Metathesis over a WO<sub>x</sub>/SiO<sub>2</sub> Catalyst: A Computational Perspective. *J. Phys. Chem. C* 2024. <https://doi.org/10.1021/acs.jpcc.4c01305>.

(32) Boudart M, Djéga-Mariadassou G. Kinetics of heterogeneous catalytic reactions. (Princeton Univ. Press, 2014).

(33) Chauvin Y, Commereuc D. Chemical counting and characterization of the active sites in the rhenium oxide/alumina metathesis catalyst. *J. Chem. Soc., Chem. Commun.*, 1992, 462-464.

The data that support the findings of this study are available from the corresponding author upon reasonable request. The following datasets are included:

- **Experimental Data:** Raw spectroscopy data (.csv files and .xlsx files). These files are available upon request.
- **Supporting Information:** Additional data, including detailed experimental procedures, supplementary figures, and tables (.pdf files). These files are available upon request.